doi:10.3788/gzxb20144308.0823006

三种不同结构的无透镜鬼成像实验研究

薛玉郎,万仁刚,冯飞,姚银萍,张同意
(中国科学院西安光学精密机械研究所 瞬态光学与光子技术国家重点实验室,西安 710119)

摘 要:为实现远距情况下的实际应用,对赝热源鬼成像进行了从透射到反射的实验研究.首先利用CCD的两个独立区域分别探测参考光和信号光,得到双缝的透射型鬼成像,继而利用一个CCD和一个独立的桶探测器分别探测参考臂和物臂的光强信息,通过对没有空间分布的物臂光强和没有经过物体而有空间分布的参考臂光强信号进行关联计算实现透射和反射鬼成像.为设计和研制能进行现场应用的样机系统,以透射结构为例,对成像结果与系统各参数之间的关系进行了详细的对比实验研究,结果表明通过增加采样率、增大光强、适当调节快门时间和光阑大小可以提高成像的分辨率和可见度.

关键词:无透镜鬼成像;赝热光源;二阶关联计算;透射成像;反射成像
中图分类号:O431.2;O431.1 **文献标识码**:A **文章编号**:1004-4213(2014)08-0823006-6

Lensless Ghost Imaging Experiments in Three Different Configurations

XUE Yu-lang, WAN Ren-gang, FENG Fei, YAO Yin-ping, ZHANG Tong-yi
(*State Key Laboratory of Transient Optics and Photonics, Xi'an Institute of Optics and Precision Mechanics, Chinese Academy of Sciences, Xi'an* 710119, *China*)

Abstract: To achieve stand-off sensing applications, ghost imaging experiments with pseudothermal light were performed from transmissive to reflective cases. First, ghost images of a transmissive double-slit aperture were retrieved in a setup that both the reference beam and signal beam were collected with two different regions of a single CCD. Then a CCD and a separate bucket detector were used to record the light intensity information of the reference beam and the signal beam, respectively. By calculating the intensity correlation function of the signal beam with no spatial light distribution and the spatial dependent reference beam that does not interact with the object, ghost images of a transmissive object and a reflective object were achieved. In order to design and develop prototype systems field applicable, detailed experimental investigations were performed to compare the effect of system parameters on the quality of imaging in the transmission configuration. The results show that enough high power of light source, large sample numbers, and proper exposure time and spatial frequency bandwidth can lead to ghost image with good resolution and visibility.

Key words: Lensless ghost imaging; Pseudothermal light source; Second-order correlation; Transmissive imaging; Reflective imaging
OCIS Codes: 110.2970; 110.3010; 110.2990; 110.3000

0 Introduction

Since the first experiment was implemented by Shih's group using spatially entangled photon pairs[1], ghost imaging has inspired much interest[2] on account of its potential applications, such as quantum lithography[3-5], quantum holography[6], quantum optical coherence tomography[7], and lensless imaging[8-12]. In ghost imaging the object image is retrieved by using the intensity correlation function of two spatially correlated

Foundation item: The National Natural Science Foundation of China (Nos. 61176084, 11204367, 11174282), the China Postdoctoral Science Foundation funded project under Grant (No. 2012M512040), and the "Western Light" Talent Cultivation Plan of Chinese Academy of Sciences

First author: XUE Yu-lang (1987—), male, master degree candidate, mainly focuses on quantum imaging technology. Email: xueyulang@opt.cn

Supervisor (Contact author): ZHANG Tong-yi (1968—), male, Professor, Ph.D. degree, mainly focuses on quantum optics measurement and quantum imaging technology. Email: tyzhang@opt.ac.cn

Received: Nov. 11, 2013; **Accepted**: Jan. 10, 2014

beams: the reference beam, which never interacts with the object and is measured with a pixelated detector, and the signal beam, which, after illuminating the object is collected by a bucket detector with no spatial resolution. This effect was initially attributed to quantum correlations associated with entanglement in the transverse wavevectors of the twin photons[13]. But a few years later, it was shown that quantum correlations were not necessary, as a similar phenomenon can be demonstrated with a pseudothermal light source possessing classical correlations[4-5,14-17]. Although the essential of this phenomenon is still under debate for its quantum or classical origin[18-22], the ghost imaging and its relevance to application have been carving their way for advancing.

To pave the way to real applications of ghost imaging, we have explored experiments from transmissive to reflective cases and from one single device to two separate devices. In this paper, we show firstly the transmissive ghost imaging of a double-slit aperture attained in an experimental setup that both the signal beam and the reference beam are collected by a single CCD. Then, by collecting the signal beam and reference beam with a bucket detector and a CCD separately, we obtain the ghost images of transmissive stencil letters XIOPM and a reflective letter V. In particular, we investigate how the system parameters affect the image quality in the transmission configuration. All these images are obtained using pseudothermal light source made by passing a He-Ne laser through a rotating ground glass plate.

1 Transmissive ghost imaging with a single CCD

The schematic experimental setup is shown in Fig. 1. A pseudothermal light source is generated by passing a He-Ne laser beam (λ=632.8 nm) through a rotating ground glass. The rotation speed of the ground glass is controlled by a programmable step motor. The diameter of the laser illuminating off axis 5 cm on the ground glass is 2 mm. According to the equation $\tau_c = d / \omega l$ (where d is the diameter of the laser spot, ω is the angular velocity of the rotating ground glass, and l is the abaxial distance of the laser illuminating on the ground glass), the correlation time of the pseudothermal light source is set to 80 ms in our experiment by adjusting the angular velocity of the rotating ground glass. BS_1 and BS_2 are 45/55 nonpolarizing beam splitters. BS_1 divides the pseudothermal light beam into two copies and they propagate along two separate optical paths. A double-slit aperture (shown in Fig. 2(a)), with 200 μm slit width and 200 μm slit separation, is inserted into the signal path as the object to be imaged. The intensity distribution of the two beams are detected by a CCD (Andor iXon 888 EMCCD) of 1 024×1 024 pixels (the size of each pixel is 13 μm×13 μm). The CCD receiver surface is divided into two regions, region A serving as the bucket detector and B the pixelated detector, to detect the light from the signal beam and reference beam respectively. The two regions' exposure are intrinsically synchronous, so the time correlation of the light recorded by the two regions is assured without an extra trigger device. As the CCD receiver surface is only about 13 mm, another beam splitter BS_2 is used to reflect the signal beam onto the region A of CCD, without disturbing the transmission of the reference beam onto the region B. By phase compensation using a movable triangular prism (M_2), the light source is made equidistant to 40 cm from the object in the signal path and from the CCD in the reference path. The exposure time of the CCD is set to 0.6 ms, which is far shorter than the correlation time of the source. Ten thousand frames are recorded and the frames are grabbed at a rate of 10 Hz so that each frame corresponds to uncorrelated speckle pattern.

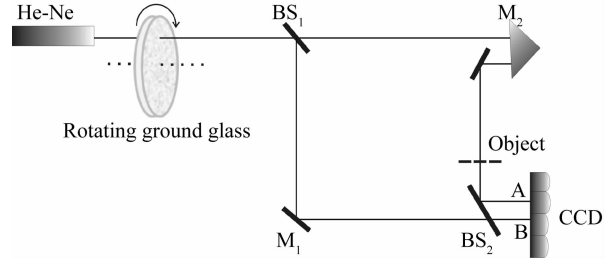

Fig. 1 The schematic setup of lensless ghost imaging of a transmissive double-slit aperture

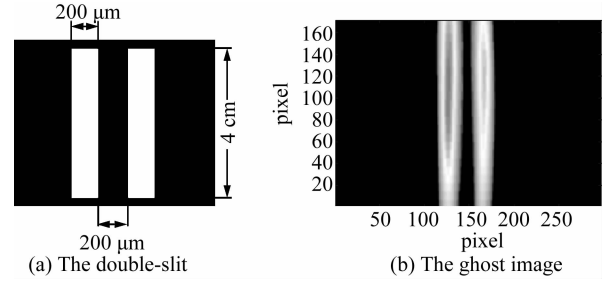

Fig. 2 The object of a double-slit aperture and its ghost image

To get the ghost image we calculate the normalized second order correlation $G^{(2)}(x,y)$ given by

$$G^{(2)}(x,y)=\frac{\frac{1}{N}\sum_{i=1}^{N}V_i I_i(x,y)}{\frac{1}{N}\sum_{i=1}^{N}V_i \cdot \frac{1}{N}\sum_{i=1}^{N}I_i(x,y)} \tag{1}$$

Here V_i, which has no spatial intensity distribution information, is the sum of the intensity recorded in the i-th frame by each pixel on region A of the CCD; $I_i(x,y)$ is the intensity distribution of the reference beam recorded in the i-th frame on region B; N equals 10 000

in this experiment. The ghost image recovered from 10 000 frames is shown in Fig. 2(b). It is an equal sized image of the object, along with a noise background.

2 Transmissive ghost imaging with a CCD and a bucket detector

In this experiment, a separate bucket detector (New Focus Model 2 031) is used to collect the light propagating in the signal path after the object. It is more convenient to build up the optical system as we do not have to collect both the reference beam and signal beam on a single CCD receiver surface of small area. We use a DAQ (data acquisition) card (Advantech PCI1716L) to convert the analog quantity produced by the bucket detector into digital data which can be analyzed by a computer. To produce ghost image, a central issue is that the light collected in the signal beam and reference beam must be correlated. So every datum got by the DAQ must be acquired in the corresponding exposure time window of the CCD. The time consumed to acquire a datum by the DAQ is far shorter than 1 μs. Therefore if we can synchronize the beginning of the exposure time of every CCD frame and the acquisition time of every DAQ datum, the datum got by the DAQ would be in the exposure time window of the CCD. Figure 3 shows the schematic illustration of the synchronization. We make use of a TTL pulse generator to produce trigger signals and set the beginning of the exposure time of the CCD and the acquisition time of the DAQ to be enabled by the rising edge of the TTL pulses. Then every frame is correlated to the datum acquired by the DAQ.

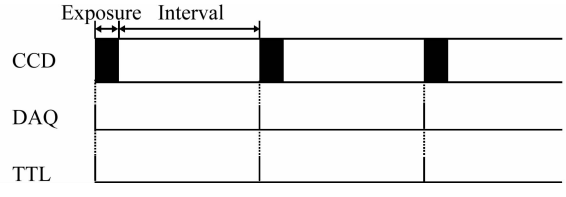

Fig. 3 The schematic illustration of the synchronization of the CCD and DAQ

The schematic and experimental setup is shown in Fig. 4. The lens and stops are used to control the transverse size of the beams and find the correlated speckles to illuminate the CCD and the object (as the CCD receiver surface is small, we must find and record the speckles in the reference beam which are correlated with the ones illuminating the object in the signal beam). The object used in this experiment is shown in Fig. 5(a). It is a stencil with transmissive letters XIOPM (which is made by etching the letters on a metal film coated glass). The hollow width of each letter is 100 μm and the letters occupy a 4.8 mm long and 1.2 mm wide rectangular space. The object and CCD are located 15 cm far from the beam splitter BS in the signal beam and reference beam, respectively. The bucket detector collects all the light transmitted through the stencil. Substituting the data V_i acquired by the DAQ and the reference beam intensity distribution $I_i(x,y)$ recorded in the CCD frames into Eq. (1), we can get the ghost image of the object.

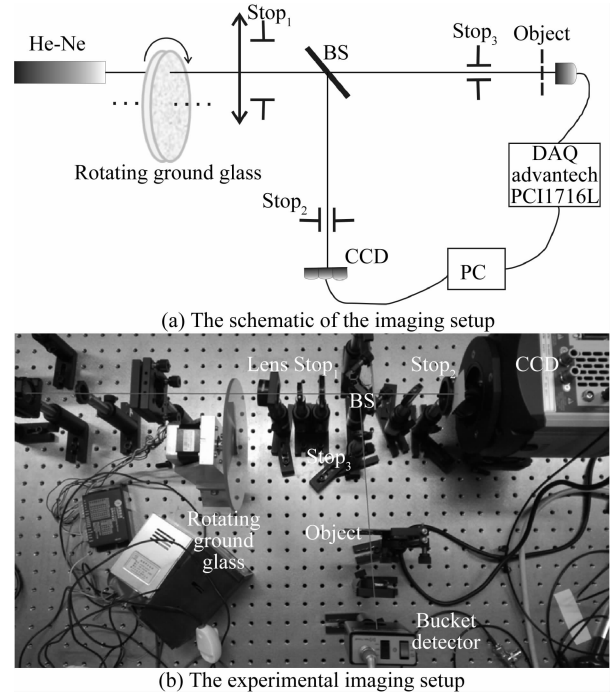

Fig. 4 The schematic and experimental setup of lensless ghost imaging of transmissive stencil letters XIOPM

To lay the foundation for the reflective experiment below and further stand-off sensing applications, we consider how the system parameters affect the image quality. First, we set the aperture size of $stop_1$ to be 10 mm and $stop_2$ ($stop_3$) to be 7 mm. The intensity of light illuminating on the object is 48.8 μW and on the CCD is 104.5 nW (we attenuate the intensity of the light sufficiently to avoid any saturation to protect the CCD, as the CCD is ultra-sensitive). When the exposure time of each frame is 0.6 ms and measurement interval is 100 ms, the images recovered from 3 000, 7 000, 10 000, and 20 000 frames are shown in Fig. 5(b)~(e), respectively. The arithmetical average we used in Eq. (1) is to approximate the ensemble average, so it naturally requires a large number of frames to make the visibility better. However, 10 000 frames are enough to get a clear image of the object in our experiment, so we take 10 000 frames for all the following experiments.

If the exposure time we set is very short, the CCD vertical smearing would become very serious and bring extra noise into every frame. The image is blurred just as shown in Fig. 6(a) when the exposure time is 0.1 ms and the measurement interval is 100 ms. But the exposure time can't be set too long either. Fig. 6(b)

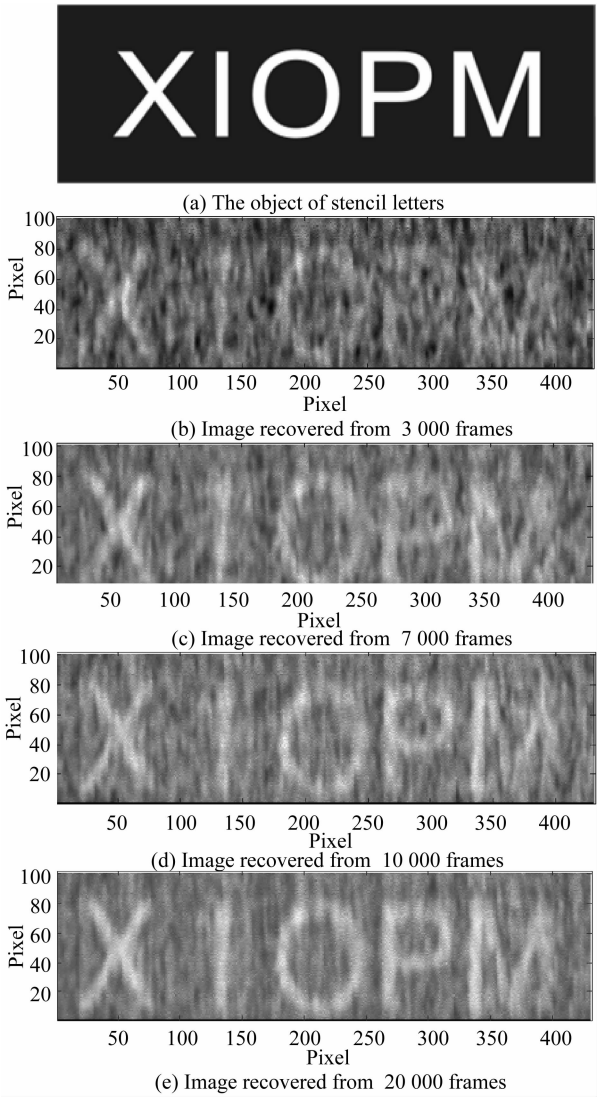

Fig. 5 The stencil of transmissive letters XIOPM and its ghost image recovered from different numbers of frames

shows the image obtained when the exposure time is 2 ms. The image is distorted because the speckles recorded during the exposure time become strips as the ground glass is rotating. To make a good approximation of the ensemble average, the frames should be recorded with measurement intervals longer than the source′s correlation time. The image shown in Fig. 6(c) is obtained when the exposure time is 0.6 ms and the interval is 30 ms, which is much shorter than the source′s correlation time. There is no surprise that it is not so clear as Fig. 5(d) where the interval is 100 ms. So, the exposure time and measurement interval time are set respectively as about 0.6 ms and 100 ms in all the experiments below.

In Ref. [23], Cheng theoretically analyzed the defocusing effect, i.e. the path between the BS and object is not equidistant to that between the BS and CCD. Figure 7(a) and (b) depict the images when the CCD is moved away by 2 cm and 4 cm further from the BS while the object is still in its original position, respectively. The image quality is degraded seriously under defocusing conditions just as what Cheng pointed out. This also demonstrates that it is an optical imaging process but not a projection process[24].

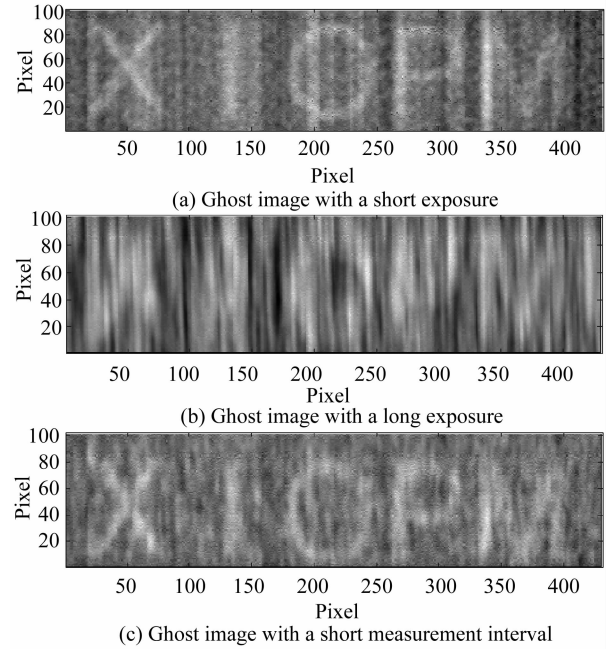

Fig. 6 The ghost image obtained when the CCD exposure time or measurement interval is changed

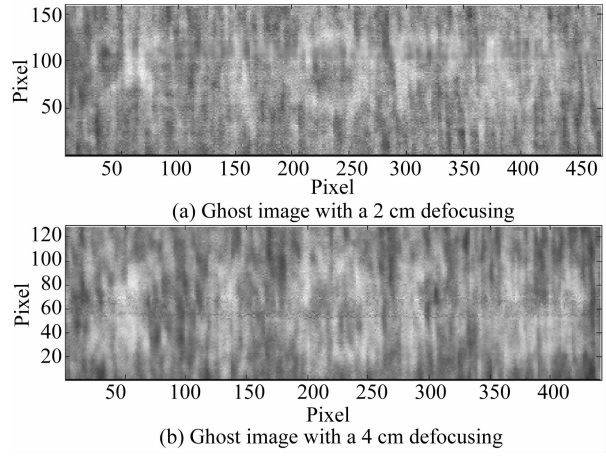

Fig. 7 The blurred images when the CCD and object are not equidistant from the BS

Figs. 8(a) and (b) show the images obtained when the size of $stop_2$ ($stop_3$) are 9 mm and 11 mm, while $stop_1$ is fixed. The stop aperture size limits the spatial frequency bandwidth of the optical transfer function to form the image[23]. The wider spatial frequency bandwidth the system permits, the better the image resolution is. The resolutions measured by a HBT type experiment under conditions correspond to Fig. 5(d), 8(a), and 8(b) are shown in Fig. 8(c). The resolution gets better when the aperture size is larger. But the visibilities of Figs. 5(d), 8(a), and 8(b) are 0.15%, 0.12%, and 0.10%, respectively, which get worse as the aperture size is

increased. So we have to make a trade-off between the resolution and visibility when we choose the stop aperture size. If the detail of the object is not so important to us or we have got enough information about it, we can improve the visibility by using a small aperture stop.

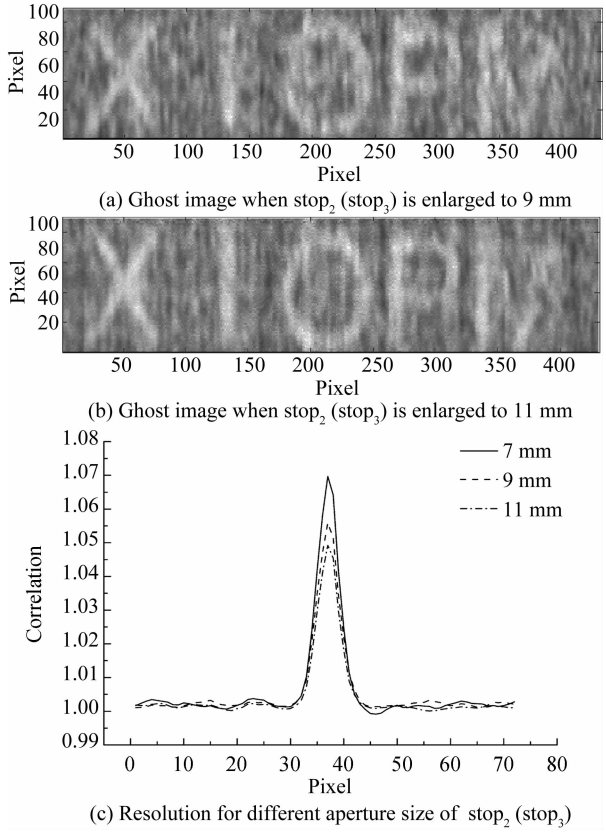

Fig. 8 The ghost images and their resolution

The image got with a higher intensity reference beam (182.4 nW) is shown in Fig. 9(a). Fig. 9(b) shows the image obtained when the intensities of the reference and signal beams are attenuated to 21.09 nW and 7.356 μW respectively. From Eq. (1), we can see the light intensity won't affect the image quality supposing that the detectors are ideal. But all real photodetectors will bring noise to their measurement. According to Fig. 9(b), if the intensity is very low, the image quality will be degraded as the detector noise dominates the measurement. By comparing Fig. 5(d) and 9(a), it is clearly that the image quality will hardly be affected by the light intensity when it is high enough. So, to obtain an image of good quality, low intensity illumination should be avoided.

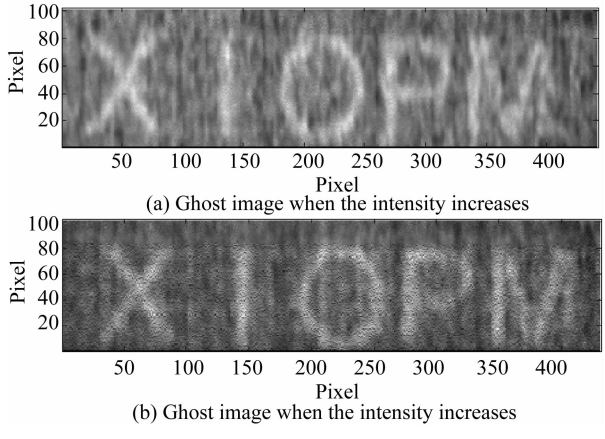

Fig. 9 Ghost images with different light intensities

3 Reflective ghost imaging with a CCD and a bucket detector

To make the experiment closer to real sensing applications, we should go forward to the case with reflective object. The object that where letter V reflects light and the part elsewhere absorbs is shown in Fig. 11(a). It is made by hollowing out the letter on a little sheet of black paper and then attaching it onto a mirror. The hollow width is about 1 mm and the whole letter is about 3 mm wide and 4 mm long. Limited by the sensitivity of the bucket detector, the light reflected by the black paper would have little influence on the imaging of the letter V.

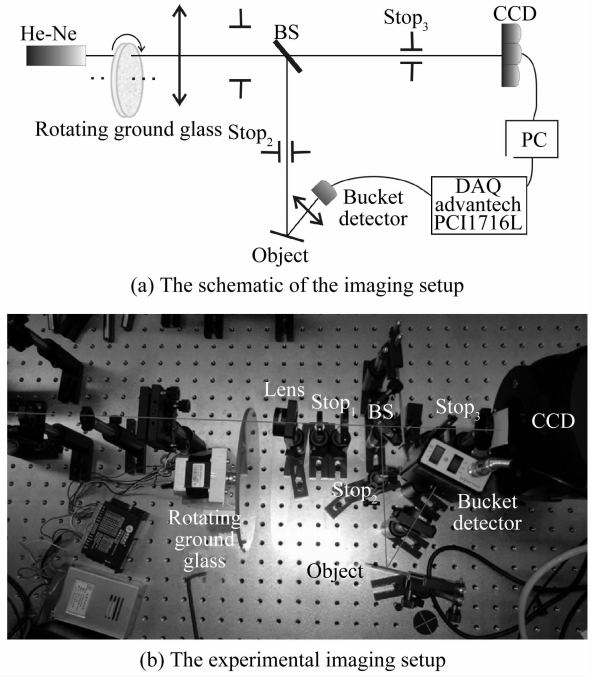

Fig. 10 The schematic and experimental setup of reflective lensless ghost imaging of the letter V

The schematic and experimental setup is shown in Fig. 10. The lens and stops are also used to control the transverse size of the beams and find the correlated speckles to illuminate the CCD and the object. The two correlated light beams propagate 15 cm from where they are splitted on the beam splitter and then illuminate on the object and CCD respectively. The bucket detector collects all the light reflected by the object. The CCD exposure time is 0.4 ms and 10 000 CCD frames with 10 000 DAQ data are recorded triggered just as that in the transmissive lensless ghost imaging of stencil letters XIOPM.

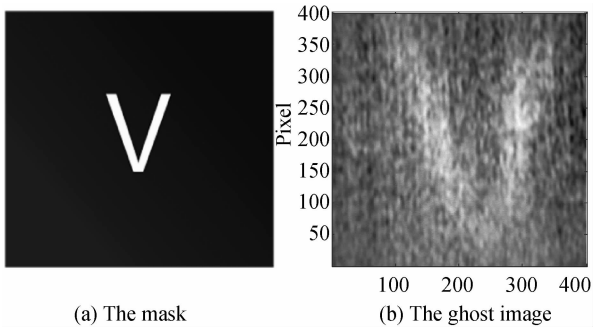

Fig. 11 The mask of a reflective letter V imaged and its ghost image

After calculating the normalized second order correlation $G^{(2)}(x, y)$ as what is done in the transmissive lensless ghost imaging of stencil letters XIOPM, we obtain the ghost image shown in Fig. 11(b). As the handmade line of the letter is not so straight, the image of the line also bends as the object do. Because the intensity of the speckles at the edge are lower than that at the center while the noise of the CCD is even-distributed, the part of the image at the center is clearer than that at the edge.

4 Conclusions

In conclusion, we have investigated ghost imaging of a transmissive double-slit aperture in a simple configuration that both the reference beam and signal beam are detected with two regions of a single CCD. After synchronous triggering the CCD and a DAQ card, transmissive ghost image of stencil letters XIOPM is recovered in a configuration that the signal beam and reference beam are detected separately by a CCD and a separate bucket detector. Especially, how the system parameters set in the experiment affect the image quality is investigated in the transmission configuration. To pave the way to real stand-off sensing applications, reflective ghost imaging of a letter V in the separate CCD and bucket detector is also performed. All the images are recovered with sufficient quality and are equal sized of the objects.

Reference

[1] PITTMAN T B, SHIH Y H, STREKALOV D V, *et al*. Optical imaging by means of two-photon quantum entanglement[J]. *Physical Review A*, 1995, **52**(5): R3429-R3432.

[2] GATTI A, BRAMBILLA E, LUGIATO L A. Quantum imaging[J]. *Progress in Optics*, 2008, **51**: 251-348.

[3] ANGELO M D, CHEKHOVA M V, SHIH Y H. Two-photon diffraction and quantum lithography[J]. *Physical Review Letters*, 2001, **87**(1): 013602.

[4] XIONG J, CAO D Z, HUANG F, *et al*. Experimental observation of classical subwavelength interference with a pseudothermal light source[J]. *Physical Review Letters*, 2005, **94**(17): 173601.

[5] ZHAI Y H, CHEN X H, ZHANG D, *et al*. Two-photon interference with true thermal light[J]. *Physical Review A*, **72**(4): 043805.

[6] ABOURADDY A F, SALEH B E A, SERGIENKO A V, *et al*. Quantum holography[J]. *Optics Express*, 2001, **9**(10): 498-505.

[7] NASR M B, SALEH B E A, SERGIENKO A V, *et al*. Demonstration of dispersion-canceled quantum-optical coherence tomography[J]. *Physical Review Letters*, 2003, **91**(8): 083601.

[8] VALENCIA A, SCARCELLI G, ANGELO M D, *et al*. Two-photon imaging with thermal light[J]. *Physical Review Letters*, 2005, **94**(6): 063601.

[9] CAO D Z, XIONG J, WANG K G. Geometrical optics in correlated imaging systems[J]. *Physical Review A*, 2005, **71**(1): 013801.

[10] CAI Y J, WANG F. Lensless imaging with partially coherent light[J]. *Optics Letters*, 2007, **32**(3): 205-207.

[11] YAO Y P, WAN R G, XUE Y L, *et al*. Positive-negative nonlocal lensless imaging based on statistical optics[J]. *Acta Physica Sinica*, 2013, **62**(15): 154201.

[12] CHEN X H, LIU Q, LUO K H, *et al*. Lensless ghost imaging with true thermal light[J]. *Optics Letters*, 2009, **34**(5): 695-697.

[13] ABOURADDY A F, SALEH B E A, SERGIENKO A V, *et al*. Role of entanglement in two-photon imaging[J]. *Physical Review Letters*, 2001, **87**(12): 123602.

[14] SCARCELLI G, VALENCIA A, SHIH Y H. Two-photon interference with thermal light[J]. *Europhysics Letters*, 2004, **68**(5): 618.

[15] FERRI F, MAGATTI D, GATTI A, *et al*. High-resolution ghost image and ghost diffraction experiments with thermal light[J]. *Physical Review Letters*, 2005, **94**(18): 183602.

[16] GATTI A, BACHE M, MAGATTI D, *et al*. Coherent imaging with pseudo-thermal incoherent light[J]. *Journal of Modern Optics*, 2006, **53**(5-6): 739-760.

[17] BACHE M, MAGATTI D, FERRI F, *et al*. Coherent imaging of a pure phase object with classical incoherent light[J]. *Physical Review A*, 2006, **73**(5): 053802.

[18] SCARCELLI G, BERARDI V, SHIH Y H. Can two-photon correlation of chaotic light be considered as correlation of intensity fluctuations[J]. *Physical Review Letters*, 2006, **96**(6): 063602.

[19] GATTI A, BONDANI M, LUGIATO L A, *et al*. Comment on "Can two-photon correlation of chaotic light be considered as correlation of intensity fluctuations?"[J]. *Physical Review Letters*, 2007, **98**(3): 039301.

[20] SCARCELLI G, BERARDI V, SHIH Y H. Scarcelli, berardi, and shih reply[J]. *Physical Review Letters*, 2007, **98**(3): 039302.

[21] ERKMEN B I, SHAPIRO J H. Unified theory of ghost imaging with Gaussian-state light[J]. *Physical Review A*, 2008, **77**(4): 043809.

[22] WANG L G, QAMAR S, ZHU S Y, *et al*. Hanbury Brown-Twiss effect and thermal light ghost imaging: A unified approach[J]. *Physical Review A*, 2009, **79**(3): 033835.

[23] CHENG J. Transfer functions in lensless ghost-imaging systems[J]. *Physical Review A*, 2008, **78**(4): 043823.

[24] SHI Y H. The physics of ghost imaging[C]. Costa N, Cartaxo A. Advances in Lasers and Electro Optics. Croatia: INTECH, 2010: 838.